Supplementary Material (ESI) for Chemical Communications

Electronic Supplementary Information (ESI) for:

Preparation of graphene relying on porphyrin exfoliation of graphite

Jianxin Geng, Byung-Seon Kong, Seung Bo Yang and Hee-Tae Jung*

National Research Laboratory, Department of Chemical and Biomolecular Engineering (BK-21), Korea Advanced Institute of Science and Technology, 373-1 Guseong-dong, Yuseong-gu, Daejeon 305-701, Korea

Contents:

S1. Experimental

Preparation of Graphene. In a general procedure, the graphene was prepared by dispersing graphite (Graphit Korpfmühl AG, 0.1 $mg \cdot ml^{-1}$) in solutions of porphyrin (0.1 $mg \cdot ml^{-1}$) in NMP containing TBA (Sigma-Aldrich, 40 wt% in water, 10 $mg \cdot ml^{-1}$). In control experiments, equal quantities of graphite were dispersed in NMP. After ultra-sonication for 30 min, the suspensions were allowed to stand for *ca*. 1 week to allow the graphite to be intercalated and exfoliated by the organic ammonium ions and porphyrin molecules. The resulting dispersions were subjected to centrifugation at 500 rpm for 90 min in order to separate the unexfoliated graphite by decanting the supernatants. The volume of the obtained supernatant and the weight of the unexfoliated graphite in the precipitate, after dried, were carefully measured and used to calculate the concentration of the graphene in the supernatant.

Graphite was dispersed in NMP, a TBA solution in NMP, a porphyrin-**3** solution in NMP, and a porphyrin-**3**/TBA solution in NMP. The supernatants obtained by centrifugation at 500 rpm for 90 min, immediately after the dispersions are prepared, show undetectable changes in colour compared to

the solvent or solutions in which the graphite was dispersed (Figure S1, a-1–a-4). However, the dispersion of graphite in the porphyrin-**3**/TBA solution undergoes a substantial colour change from green to black, during storage for *ca.* 1 week, indicating that the intercalation and exfoliation take place slowly. At this stage, all the dispersions were subjected to centrifugation to remove the unexfoliated graphite from the dispersions (Figure S1, b-1–b-4). In contrast to the graphene dispersion in the porphyrin-**3**/TBA solution, which undergoes a substantial change in colour (Figure S1, b-4 vs. a-4), the graphene dispersion in TBA solution shows little colour change (Figure S1, b-3 vs. a-3), and no change in colour for the graphene dispersions in NMP and in porphyrin-**3** solution (Figure S1, b-1 vs. a-1; b-2 vs. a-2). Therefore, we conclude that either organic ammonium ion alone or porphyrin alone is not efficient to disperse graphite, and the dispersibility of graphene in NMP alone is very poor.

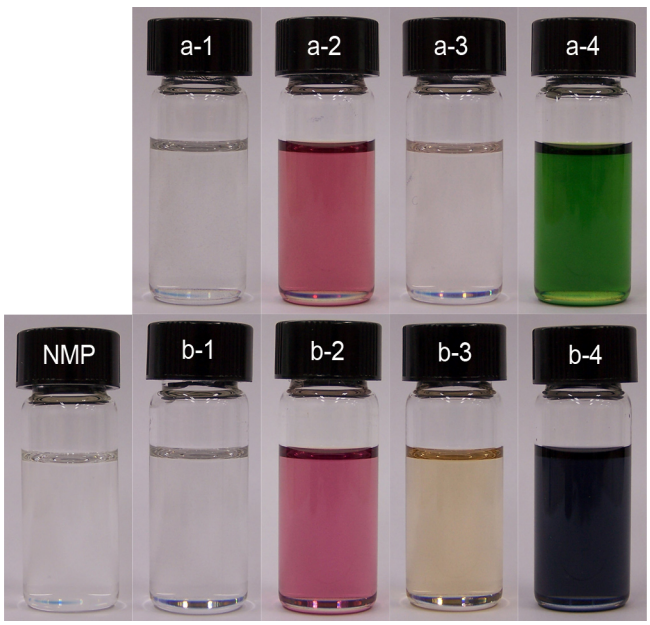

Figure S1. Optical images of graphene solutions. The bottles in the upper row contain supernatants obtained by centrifugation of graphite dispersions immediately after they were prepared. The bottles in the lower row show the supernatants obtained by centrifuging graphite dispersions 1 week after they are prepared; (1) graphene dispersion in NMP, (2) graphene dispersion in a porphyrin-**3** solution in NMP, (3) graphene dispersion in a TBA solution in NMP, (4) graphene dispersion in a porphyrin-**3**/TBA solution in NMP, and (NMP) pure NMP solvent.

Characterization of Graphene. UV-visible spectra were recorded using a JASCO V-570 spectrophotometer. The supernatant of the graphite dispersion in NMP was measured as it was obtained, while the other solutions and supernatants were measured after diluted by a factor of 20. TEM images were obtained on a JEOL JEM-2100F TEM operated at 200 kV. TEM samples were

prepared by casting the graphene supernatant on a surface of a 25 wt% NaCl aqueous solution, resulting in the formation of a porphyrin/graphene film on the surface, with fast dissolving of NMP and TBA in water. The film was picked up with copper holey grids. The residual NaCl and porphyrin-**3** on the sample surfaces were removed by floating the grids on water and chloroform surfaces. Raman spectroscopic analysis of graphene was carried out by using a high resolution dispersive Raman microscope (HORIBA Jobin Yvon HR800 UV) with an excitation laser of 514. The samples for Raman measurement were prepared on glass substrates by a vacuum filtration method. In brief, graphene films were deposited on the surfaces of AAO membranes through vacuum filtration, during which process the films were repeatedly washed with copious amounts of NMP. After drying at 60 ^{o}C for *ca.* 0.5 h, the graphene films were transferred to glass surfaces. Finally, the graphene samples were dried over night at 60 ^{o}C in a vacuum oven before measurement. AFM images were obtained using an SPA 3800N microscope with a SPA-400 scanner.

S2. **A Schemetic for Exfoliation Mechanism**

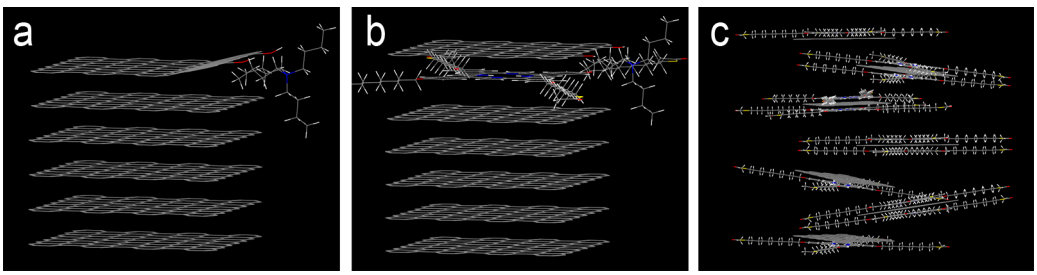

Figure S2. A schematic for the dispersing mechanism: (a) selective interaction of TBA with the hydroxyl groups at graphite edges, (b) porphyrin molecules exfoliating graphene sheets after the sheets have been wedged up, and (c) graphene sheets dispersed in NMP, with porphyrin molecules coating on the surfaces.

The observation that graphene is efficiently produced only when both porphyrins and organic ammonium ions are present in a NMP solution can be explained by operation of a two-step process involving an organic ammonium ion interaction and porphyrin induced exfoliation. It has been reported that hydroxyl groups are present on graphite edge surfaces.[S1] Thus, TBA ions prefer to interact with the hydroxyl groups on the edges of graphite particles as a consequence of dipole-dipole interactions (Figure S2a).[S2] Once the graphene edges interact with TBA, porphyrin molecules are likely to exfoliate graphene sheets via a π-π interaction (Figure S2b). The UV-visible spectroscopic data described in the paper (Figure 1c) support this proposal. Consequently, graphene sheets are produced as a suspension in NMP with the aid of the porphyrin (Figure S2c).

S3. **Additional TEM Images of Graphene Sheets**

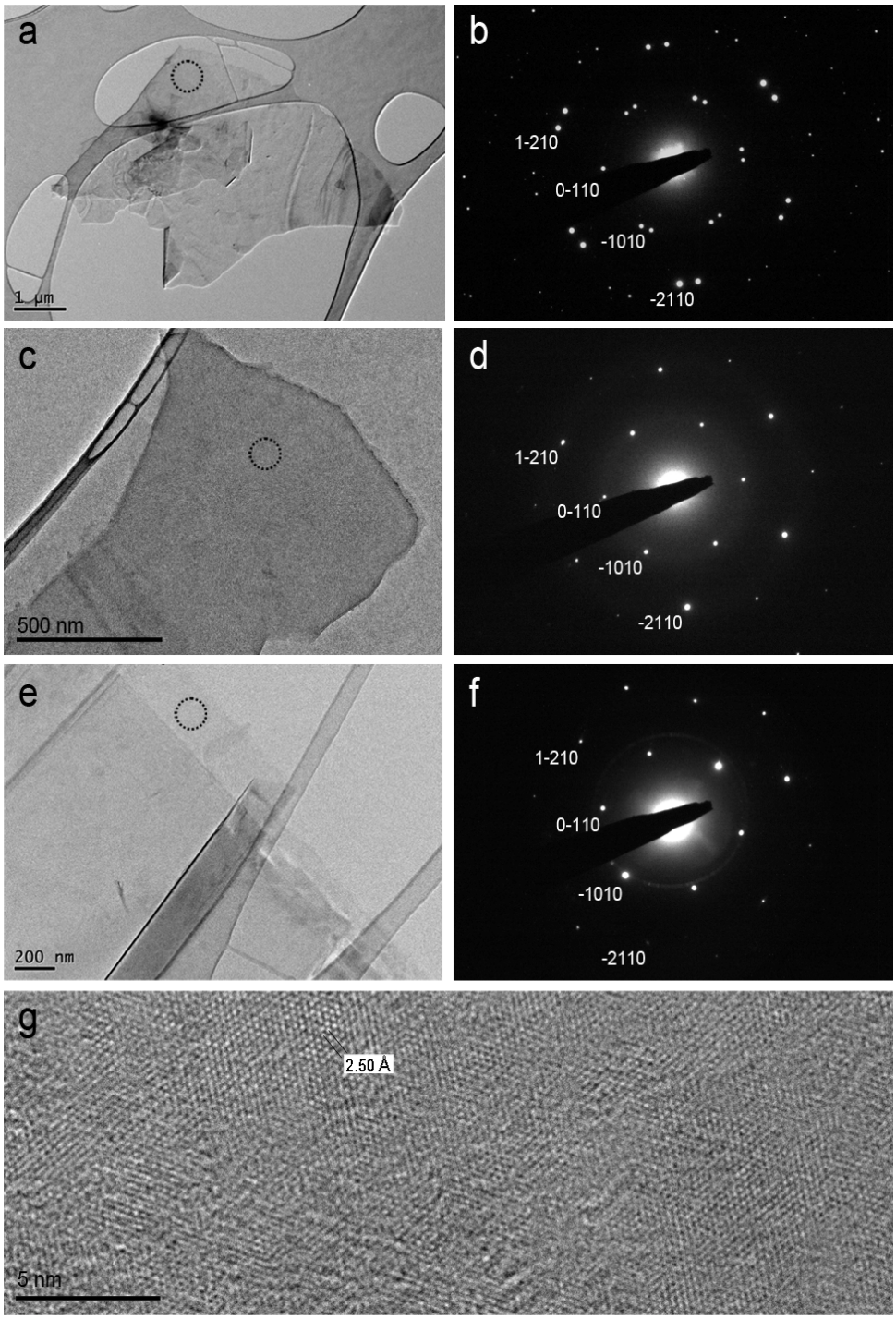

Figure S3. TEM characterization of graphene: (a) an image of a few-layer graphene sheet, (b) the ED pattern obtained from the circle-marked area in panel a, (c) an image of a few-layer graphene sheet, (d) the ED pattern obtained from the circle-marked area in panel c, (e) an image of a single-layer graphene sheet, (f) the ED pattern obtained from the circle-marked area in panel e, and (g) a HRTEM image obtained from the circle-marked area of the graphene sheet in panel e.

In order to further elucidate the structures of the graphene sheets prepared using this new methodology, additional TEM images of graphene sheets are provided (Figure S3). In Figure S3a and c are shown two examples of few-layer graphene sheets, which are determined by corresponding ED patterns (Figure S3b, d). The ED patterns were recorded from the circle-marked regions of the graphene sheets, in which spots (0-110) and (-1010) are weaker in intensity than spots (1-210) and (-2110), indicating the few-layer feature of the graphene sheets (Figure S3a, c).[S3] In addition, Figure S3b contains two sets of ED patterns because overlapped few-layer graphene sheets with an orientation angle have been used for ED patterning. In Figure S3e is shown an image of a single-layer graphene sheet, with its corresponding ED pattern, which is obtained from the circle-marked region, displayed in Figure S3f. In the ED pattern, spots (0-110) and (-1010) are more intense than spots (1-210) and (-2110), indicating the single-layer feature of the graphene sheet.[S3] Furthermore, lattice image of graphene sheets is readily observed when the graphene surfaces are relatively clean, i.e., less quantity of amorphous materials is absorbed on the layers. A high-resolution TEM (HRTEM) image (Figure S3g), which is obtained from the circle-marked area in Figure S3e, shows the presence of a highly ordered hexagonal lattice with a measured spacing of 0.25 nm, which corresponds to the centre-to-centre distance of two graphene unit cells. The existence of highly ordered hexagonal lattice verifies the perfection of sp^2 carbon network in the graphene prepared by using the new methodology.

S4. AFM Observation of Graphene Sheets

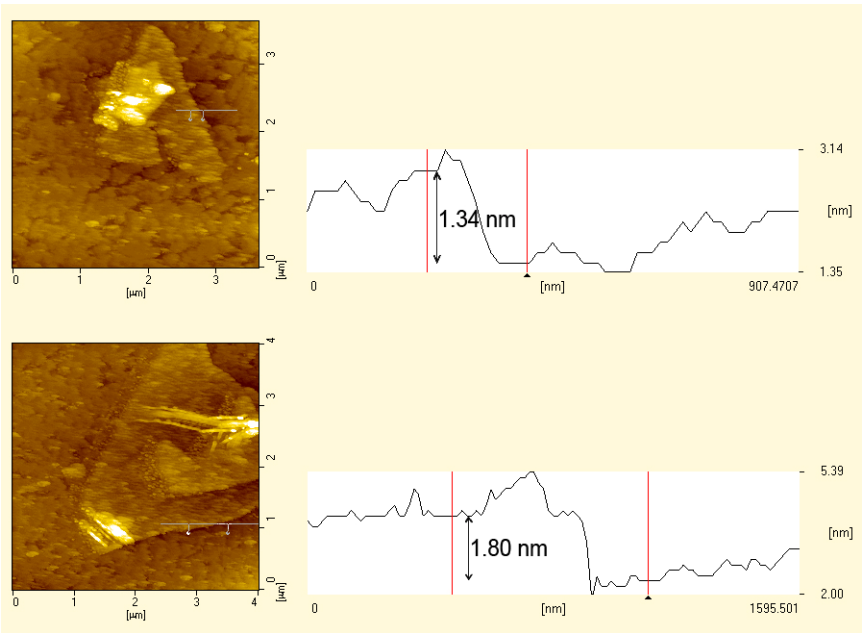

Figure S4. AFM images of the graphene sheets.

Isolated graphene sheets were coated on mica surfaces by spraying method. The films were repeatedly rinsed with DI water to remove the TBA during spraying process. Basically, this method can prepare graphene and carbon nanotube films on any substrate, as well as films with various thicknesses by changing the suspension volume applied for film preparation.[S3,S4] AFM was used to observe the morphology of the graphene sheets. In Figure S4 are shown two typical images of graphene sheets with lateral dimension of microns, in agreement with the TEM observation. Cross sectional analysis shows that the graphene sheets have thickness of 1.34 and 1.80 nm, respectively. The interlayer distance in bulk graphite is *ca*. 0.34 nm, implying that the graphene sheets shown in Figure S4 are few-layer entities given that the sheets are sandwiched by porphyrin molecules, ideally, with one porphyrin monolayer being *ca*. 0.3 nm thick.[S5] However, graphene films with theoretical thickness are rarely found due to the facts that at such high resolution the apparent thickness obtained by AFM includes the chemical and van der Waals contrast, that there may be a layer of absorbed water or solvent between the graphene sheets and substrate, and that instrumental offset of *ca*. 0.5 nm always exist, which is even greater than the thickness of a single-layer graphene.[S6,S7] These three factors lead to overestimating the actual thickness of graphene sheets. Therefore, single-layer graphene sheets with thickness of *ca*. 1 nm have commonly been reported.[S3,S6,S8] Keeping these complicated factors in mind, we conclude that the graphene sheets (Figure S4) can contain 1, 2, or 3 layers.

S5. Optical Images of Graphene Sheets Used for Raman Measurement

Raman spectroscopic analysis of graphene was carried out by using a high resolution dispersive Raman microscope, which enable us to precisely position samples on the base of the different color and contrast of the graphene sheets with varying thickness under the optical microscope.[S9] In Figure S5 are shown the in situ images of graphene sheets where the corresponding Raman spectra in the paper (Figure 3) were recorded. The green spots show the position where the laser shined on.

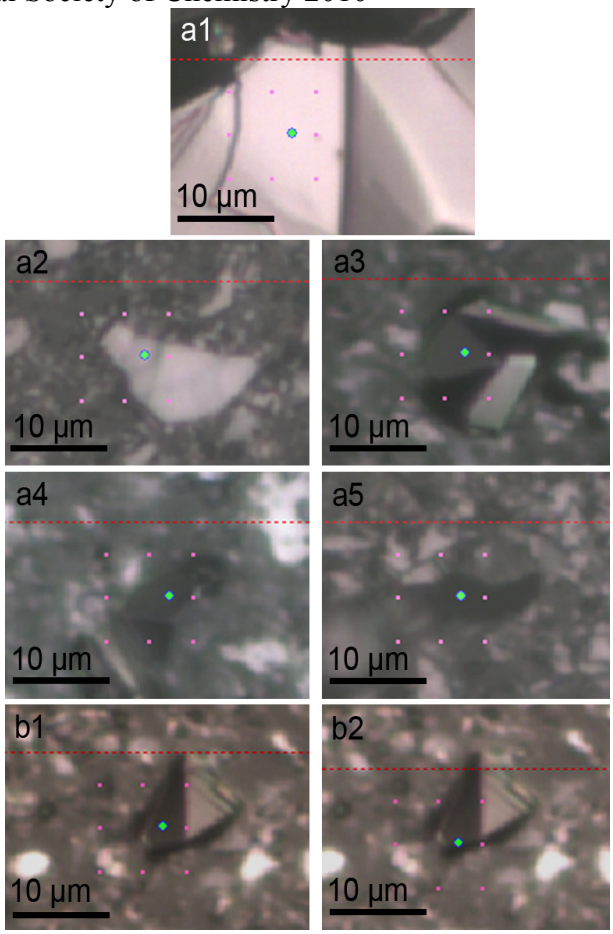

Figure S5. Optical images of graphene sheets used for Raman measurement. The number designated to each panel corresponds to the line number in Figure 3 in the paper.

S6. FT-IR spectra of graphene

The porphyrin molecules on graphene surfaces can be removed by heat treatment. In fact, we tested FT-IR spectra of the porphyrin-hybridized graphene before and after heat treatment. The samples used for FT-IR measurement were prepared on surfaces of silicon wafer by vacuum filtration method. The presence of porphyrin molecules on graphene surfaces can be confirmed by FT-IR spectroscopy. In Figure S6 are shown the FT-IR spectra of graphene films before and after thermal annealing at 400 ^{o}C for 2 h in vacuum. Before thermally annealed, the graphene film provides a spectrum containing characteristic peaks at around 2900 cm^{-1} ascribed to the stretching vibrations of C-H bonds of the substituent groups of porphyrin-**3**, implying the presence of porphyrin molecules on the surfaces of graphene sheets. In contrast, these peaks are disappeared once the graphene film has been thermally annealed, indicating the removal of the porphyrin molecules from the graphene surfaces. On the other hand, porphyrin molecules attached on graphene surfaces could be of an advantage. For example, the

graphene/porphyrin hybrid could be used in photoelectrochemical application because of the unique photochemical properties of the porphyrin.[S10]

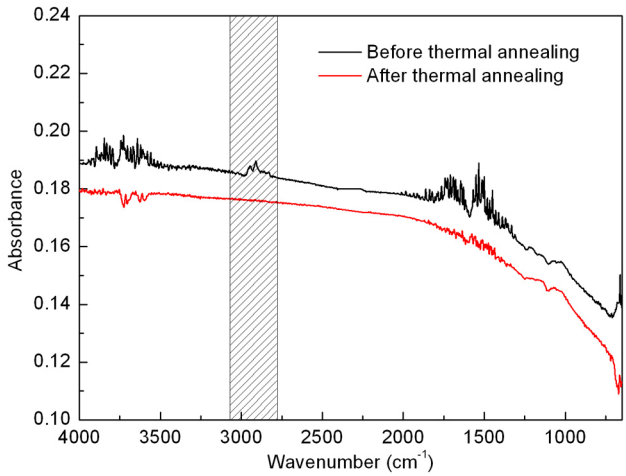

Figure S6. FT-IR spectra of graphene films before and after thermally annealed at 400 ^{o}C for 2h in vacuum.

References:

[S1] M. Nakahara, Y. Sanada, *J. Mater. Sci.* **1995**, *30*, 4363-4368.

[S2] Z.-H. Liu, Z.-M. Wang, X. Yang, K. Ooi, *Langmuir* **2002**, *18*, 4926-4932.

[S3] Y. Hernandez, V. Nicolosi, M. Lotya, F. M. Blighe, Z. Sun, S. De, I. T. McGovern, B. Holland, M. Byrne, Y. K. Gun'ko, J. J. Boland, P. Niraj, G. Duesberg, S. Krishnamurthy, R. Goodhue, J. Hutchison, V. Scardaci, A. C. Ferrari, J. N. Coleman, *Nat. Nanotech.* **2008**, *3*, 563-568.

[S4] E. Artukovic, M. Kaempgen, D. S. Hecht, S. Roth, G. Grüner, *Nano Lett.* **2005**, *5*, 757-760.

[S5] X. Qiu, C. Wang, Q. Zeng, B. Xu, S. Yin, H. Wang, S. Xu, C. Bai, *J. Am. Chem. Soc.* **2000**, *122,* 5550-5556.

[S6] K. S. Novoselov, A. K. Geim, S. V. Morozov, D. Jiang, Y. Zhang, S. V. Dubonos, I. V. Grigorieva, A. A. Firsov, *Science* **2004**, *306*, 666-669.

[S7] A. Gupta, G. Chen, P. Joshi, S. Tadigadapa, P. C. Eklund, *Nano Lett.* **2006**, *6*, 2667-2673.

[S8] S. Stankovich, D. A. Dikin, G. H. B. Dommett, K. M. Kohlhaas, E. J. Zimney, E. A. Stach, R. D. Piner, S. T. Nguyen, R. S. Ruoff, *Nature* **2006**, *442*, 282-286.

[S9] Z. H. Ni, H. M. Wang, J. Kasim, H. M. Fan, T. Yu, Y. H. Wu, Y. P. Feng, Z. X. Shen, *Nano Lett.* **2007**, *7*, 2758-2763.

[S10] T. Umeyama, M. Fujita, N. Tezuka, N. Kadota, Y. Matano, K. Yoshida, S. Isoda, H. Imahori, *J. Phys. Chem. C* **2007**, 111, 11484-11493.